J Opt
https://doi.org/10.1007/s12596-024-01752-x

RESEARCH ARTICLE

# Design optimization of Yb-doped fiber lasers for operation in radiation environments

**Mengmeng Tao[1,2] · Yamin Wang[1] · Ke Wang[1] · Hongwei Chen[1] · Jingfeng Ye[1] · Yanlong Shen[1] · Dahui Wang[1] · Xisheng Ye[2]**

Received: 3 January 2024 / Accepted: 24 February 2024


**Abstract** Radiation hardening should be considered for various active fiber systems operated in adverse environments to reduce their sensitivity to complex ionizing radiations. And, architecture optimization through numerical simulation provides an efficient choice. Here, introducing radiation effects into the conventional fiber laser model, a radiation model concerning the design optimization of low- and moderate-power Yb-doped fiber lasers is developed. And, experiments at different radiation levels up to 750 Gy are carried out for validation, demonstrating the ability of this model to correctly simulate the performance of the Yb-doped fiber laser in harsh environments. Then, with this model, impacts of active fiber length, pump scheme, and pump allocation on the output characteristics of Yb-doped fiber lasers are analyzed numerically. And, optimization of Yb-doped fiber lasers are conducted through architecture design. Simulations show that a proper design with relatively short active fiber and dynamic pump allocation can remarkably improve the radiation tolerance of Yb-doped fiber lasers.

**Keywords** Radiation induced attenuation · Yb-doped fiber laser · Radiation responses

✉ Mengmeng Tao
tonylemon@yeah.net

[1] State Key Laboratory of Laser Interaction with Matter, Northwest Institute of Nuclear Technology, Xi'an 710024, China

[2] Wang Zhijiang Laser Innovation Center, Shanghai Institute of Optics and Fine Mechanics, Chinese Academy of Sciences, Shanghai 201800, China

## Introduction

As various rare-earth doped fiber systems are rapidly expanding their applications in adverse environments, their radiation responses are attracting more and more attention. And, extensive research has demonstrate that, severe power degradation appears for various fiber systems operated in radio-active environments due to the excess losses at the pump and the signal wavelengths in the irradiated active fibers [1–3].

Widely explored for space communications, Er-doped and Er/Yb co-doped fiber amplifiers are the most intensively investigated for radioactive applications. Experiments by J. Ma show that, with the active fiber exposed to γ-ray, Er/Yb co-doped fiber amplifiers experienced a remarkable gain drop of about 13 dB at 300 Gy [4]. Besides, in A. Ladaci's report, although Ce co-doping helps to improve the radiation-resistance of the Er-doped fiber, a strong gain decline of about 8 dB at 300 Gy is still recorded when the active fiber, a section of 8 m long Er-Ce codoped fiber, is irradiated by an X-ray source [5]. And, recently, a gain deterioration of about 5.5 dB at 300 Gy is witnessed for an Er-doped fiber amplifier with commercial Er-doped fibers [6]. Tm-doped fiber lasers are promising for space communication and space-borne lidar. And, the radiation effects on Tm-doped fiber lasers have also been investigated. Experiments with $^{60}$Co gamma source show that, for moderate-power (tens of Watt) Tm-doped fiber lasers, the power decline could reach up to 50% at 300 Gy [7–10].

Yb-doped fiber lasers and amplifiers exhibit similar responses. In 2009, B. Fox reported the gamma radiation effects of a low-power (within several Watt) Yb-doped fiber amplifier [11]. For an accumulated radiation dose of only 70 Gy, the amplifier experienced a remarkable power drop from 0.8 W to 0.15 W. Later, in 2022, S. Sun investigated

Published online: 13 April 2024

the response of a moderate-power Yb-doped fiber amplifier. Slope efficiency of the Yb-doped fiber amplifier drops from ~ 75% to only about 10% after the active fiber is exposed to 100 Gy of gamma radiation [12]. The situation gets even worse for high-power Yb-doped fiber lasers and amplifiers at hundreds of Watt. In 2018, experiments by Y. Wang reveal that, after exposing the Yb-doped fiber to 117 Gy of gamma radiation, the slope efficiency of a kW-level Yb-doped fiber laser shrank sharply from over 80% to about 30% [13]. Taking the elevation of lasing threshold into consideration, it can be estimated that the output power experienced a significant decline over 650 W, which would surely cause lethal damage to the laser system. Research by Y. S. Chen gives similar results for Yb-doped fiber amplifiers [14]. For radiation doses over 255 Gy, the optical–optical efficiency of the amplifier keeps below 25%, manifesting fatal performance deterioration.

To guarantee safe and efficient operation in harsh environments, a variety of measures have been proposed to improve the radiation tolerance of various fiber systems [2, 3, 15]. As the active fiber is the most radiation sensitive, the first and most widely investigated solution involves enhancing the radiation tolerance of the active fiber to decrease the radiation induced attenuation (RIA) levels at the pump and signal wavelengths. And, a plenty of methods have been investigated, including Ce-doping [5, 16–20], F-doping [20], $H_2$/$D_2$ loading [9, 10, 21–23], proportion optimization of co-doping elements [24–26], and pre-irradiation [27, 28].

In addition to these fiber treatment approaches, another solution refers to the architecture optimization of fiber systems to reduce radiation vulnerability, regardless of the fiber behavior. First proposed by S. Girard research group, hardening-by-architecture approach provides an alternative way for space-borne fiber system design [3]. And, this kind of optimization requires a simulation tool to allow the examination of different design parameters with a limited number of radiation tests.

In 2004, introducing the RIA into the classical propagation equations, O. Berne developed a model for the prediction of EDFA gain in space radiation environments [29]. Later, S. Girard's group proposed a coupled experiment/simulation approach for the design of radiation-hardened Er-dopd and Er/Yb codoped fiber amplifiers [30–32]. In this approach, firstly, based on the rate equations and the particle swarm optimization technique, a state-of-the-art numerical model is developed. Secondly, the principal input parameters of the simulation model are measured through radiation experiments. Then, the proposed simulation procedure is validated through comparisons with the measured output results of the amplifiers at both the pristine state and the irradiated state. And, finally, the verified numerical code is used to optimize the radiation resistance of the amplifiers by varying the amplifier design parameters. In 2018, L. Mescia further improved this model by taking thermal effects into account [33, 34]. And, the temperature dependence of the refractive index, emission and absorption cross sections are included. Numerical results highlight that the extra waste heat inside the active fiber could strongly deteriorate the amplifier performance.

However, up to now, most of the reported architecture optimization work is focused on Er-doped and Er/Yb dodoped fiber amplifiers aiming for space applications. Nowadays, more and more Yb-doped fiber systems are getting exploited for earth-bound applications in adverse environments, including nuclear plants and accelerators. And, related optimization work should be considered. In 2020, we developed a multiphysics thermal model concerning the radiation response of high-power Yb-doped fiber lasers [35]. Compared to the previous model for Er-doped and Er/Yb co-doped fiber amplifiers [29–34], thermal effects on lifetime, the refractive index change caused by radiation induced compaction (RIC), and the radiation induced lifetime change (RILC) are all considered. And, the simulation results fit the reported experiment records quantitatively.

However, for low- and moderate-power fiber systems, thermal effects become negligible. In fact, with an optimized active fiber length, even for kW level high power Yb-doped fiber lasers, the maximal temperature rise keeps within 100 K at 500 Gy [35, 36]. Thus, for the design optimization of low- and moderate-power Yb-doped fiber systems, the complicated thermal model can be simplified to reduce its time cost. Here, a simplified radiation model is developed, where only the primary radiation factor, namely RIA, RIC and RILC, are taken in consideration, while the secondary thermal effects are neglected. Comparisons with radiation experiments of low power Yb-doped fiber lasers show excellent consistence, demonstrating the validity of this model. Then, this validated model is used to predict the general trends of Yb-doped fiber lasers by varying different design parameters, including the active fiber length, pump scheme, and pump allocation. And, it's demonstrated that the radiation vulnerability of Yb-doped fiber lasers can be greatly reduced with an optimized architecture design.

## Modeling methodology

The basic idea of the radiation model is to introduce the major macroscopic changes of the active fiber induced by radiation into the conventional fiber laser model [37, 38].

### Conventional fiber laser model

For a two-level laser system, the population density of the excited state $N_1$ is governed by the rate equation as [37, 38]

$$\frac{dN_1(z)}{dt} = \frac{\Gamma_p \lambda_p [P_p^+(z) + P_p^-(z)]}{hcA_c}(\sigma_{ap} + \sigma_{as})[N - N_1(z)] - \frac{\Gamma_s \lambda_s [P_s^+(z) + P_s^-(z)]}{hcA_c}(\sigma_{ep} + \sigma_{es})N_1(z) - \frac{N_1(z)}{\tau} \tag{1}$$

where $N$ is the doping concentration of Yb ions. $h$ is the Planck's constant, and $c$ is the velocity of light in vacuum, while $A_c$ is the core area of the fiber. $\tau$ is the lifetime of the excited state. $\Gamma_p$ and $\Gamma_s$ are the overlapping factors of the pump and laser signal, respectively. $\sigma_{ap}$ and $\sigma_{ep}$ represent the absorption and emission cross-sections at the pump wavelength $\lambda_p$. $\sigma_{as}$ and $\sigma_{es}$ are the absorption and emission cross-sections at lasing wavelength $\lambda_s$. $P_s^{\pm}(z)$ represents the forward and backward laser signal power along the fiber, while $P_p^{\pm}(z)$ stands for the forward and backward pump power along the fiber, respectively.

At steady state, $N_1$ can be derived as

$$N_1(z) = N\frac{\frac{\Gamma_p \sigma_{ap}[P_p^+(z)+P_p^-(z)]\lambda_p}{hcA_c} + \frac{\Gamma_s \sigma_{as}[P_s^+(z)+P_s^-(z)]\lambda_s}{hcA_c}}{\frac{\Gamma_p(\sigma_{ap}+\sigma_{ep})[P_p^+(z)+P_p^-(z)]\lambda_p}{hcA_c} + \frac{\Gamma_s(\sigma_{as}+\sigma_{es})[P_s^+(z)+P_s^-(z)]\lambda_s}{hcA_c} + \frac{1}{\tau}} \tag{2}$$

In the active fiber, the propagation of the pump $P_p^{\pm}(z)$ and the laser $P_s^{\pm}(z)$, is confined by the following equation[37, 38]

$$\begin{aligned} \pm\frac{dP_p^{\pm}(z)}{dz} &= -\Gamma_p[\sigma_{ap}(N - N_1(z)) - \sigma_{ep}N_1(z)]P_p^{\pm}(z) - \alpha_p P_p^{\pm}(z) \\ \pm\frac{dP_s^{\pm}(z)}{dz} &= \Gamma_s[\sigma_{es}N_1(z) - \sigma_{as}(N - N_1(z))]P_s^{\pm}(z) - \alpha_s P_s^{\pm}(z) + \Gamma_s \sigma_{es}N_1(z)\frac{2hc^2}{\lambda_s^3}\Delta\lambda_e \end{aligned} \tag{3}$$

where $\alpha_p$ and $\alpha_s$ are the transmission loss of the fiber at the pump wavelength and the laser wavelength, respectively. $\Delta\lambda_e$ represents the spontaneous emission bandwidth.

And, the boundary conditions for propagation are

$$\begin{aligned} P_p^+(0) &= P_f + R_p^0 P_p^-(0) \\ P_p^-(L) &= P_b + R_p^L P_p^+(L) \\ P_s^+(0) &= R_s^0 P_s^-(0) \\ P_s^-(L) &= R_s^L P_s^+(L) \end{aligned} \tag{4}$$

where $P_f$ is the forward pump power at the input facet of the active fiber, and, $P_b$ is the backward pump power at the output facet. $R_p^0$ and $R_s^0$ are the reflectivities of the pump and the laser at the input facet, while $R_p^L$ and $R_s^L$ are the reflectivities of the pump and the laser at the output facet. And, $L$ is the length of the active fiber.

Together, the above equations form the conventional fiber laser model.

**Radiation effects**

Here, 3 primary radiation factors, namely RIA, RIC and RILC, are considered.

*RIA*

Among all these elements, RIA is the primary factor that should be considered. RIA corresponds to an increase of transmission loss due to radiation induced defects [3, 39].

As RIA causes extra loss in the active fiber, in the propagation equation, the overall transmission loss for the pump and the laser signal, $\alpha_p$ and $\alpha_s$, should be expressed as

$$\begin{aligned} \alpha_p &= \alpha_{p0} + \alpha_p(D) \\ \alpha_s &= \alpha_{s0} + \alpha_s(D) \end{aligned} \tag{5}$$

where $\alpha_{p0}$ and $\alpha_{s0}$ are the intrinsic loss, while $\alpha_p(D)$ and $\alpha_s(D)$ denote the radiation induced extra loss of the active fiber at radiation dose $D$.

*RIC*

RIC is another factor should be taken into account. RIC refers to the refractive index change of the fiber caused by radiation [3, 39]. And, this variation in refractive index profile would surely affect the waveguide property of the fiber core.

Experiments show that, for radiation doses within several kGy level, the refractive index change caused by radiation can be written as [40–42]

$$\begin{aligned} n_{co}(D) &= n_{co}(0) + \kappa'_{co} D\,(0 \le r \le r_1) \\ n_{cl}(D) &= n_{cl}(0) + \kappa'_{cl} D\,(r_1 < r \le r_2) \end{aligned} \tag{6}$$

where $r_1$ and $r_2$ are the radii of the core and the inner cladding, respectively. $n_{co}(0)$ and $n_{cl}(0)$ denote the refractive indexes of the core and the cladding for the pristine fiber. $\kappa'_{co}$ and $\kappa'_{cl}$ are the radiation-optic coefficients of the fiber core and the cladding, respectively.

In the rate equation and propagation equation, the overlapping factor of the laser signal, $\Gamma_s$, is calculated as

$$\Gamma_s = 1 - e^{-2\frac{r_1^2}{w^2}} \tag{7}$$

where $w$ is the mode field radius of the laser signal.

For fiber cores with a normalized frequency parameter $V$ bigger than 1.5, $w$ can derived by [43]

$$w = r_1(0.632 + 1.478V^{-3/2} + 4.76V^{-6}) \tag{8}$$

where, $V$ is directly determined by the refractive indexes of the fiber core and the cladding. In radiation environments, $V(D)$ can be attained through the following expression

$$V(D) = \frac{2\pi r_1}{\lambda_s}\sqrt{n_{co}^2(D) - n_{cl}^2(D)} \tag{9}$$

*RILC*

RILC refers to the lifetime change caused by radiation. Thus, in adverse environments, the lifetime parameter in the rate equation should be updated.

It has been demonstrated that, for radiation doses within hundreds of kGy level, the lifetime of the.$^2F_{5/2}$ energy level of Yb ions $\tau(D)$ can be written as [44, 45]

$$\tau(D) = \tau_0(1 + D)^{\gamma}, \tag{10}$$

where $\tau_0$ is the initial lifetime of Yb ions before irradiation, and $\gamma$ is the radiation-lifetime coefficient.

With all these factors considered, the conventional fiber laser model can be modified. And, the radiation model for fiber lasers with irradiated active fibers is developed.

## Validation of the model

In this part, the radiation model is validated experimentally with a low-power Yb-doped fiber laser.

### RIA measurement

First, RIA of the homemade 10/130 double-clad Yb-doped fiber is measured with the setup illustrated in Fig. 1. A 1070 nm laser source is exploited for the investigation of RIA characteristics at the laser wavelength. The laser source is lead into and out of the $^{60}$Co radiation chamber through two sections of 10 m long un-doped fiber. And, the power of the laser source is set to be at the mW level to avoid possible bleaching effects. A power-meter (PM) is utilized to monitor the propagated laser power at the output end of the passive fiber. In fact, before the experiments, γ radiation response of the un-doped fiber is also tested. And, no detectable RIA is recorded within a deposited radiation dose of 1000 Gy, eliminating the influence of the passive fiber.

The measured RIA of the Yb-doped fiber at the laser wavelength is depicted in Fig. 2. As can be found, the RIA increases monotonously with the accumulation of the radiation dose. Analysis shows that the relationship between RIA and the deposited radiation dose follows the Power Law with an expression of

$$RIA = 3.3863 \times 10^{-3} \cdot D^{0.82759} \tag{11}$$

### Radiation experiments and simulation

Then, the radiation response of a low-power Yb-doped fiber laser is investigated with the layout depicted in Fig. 3. A simple linear cavity centering at 1070 nm is built with two FBGs. And, to protect the FBGs from the radiation, a long cavity of about 26 m is exploited, consisting of 6 m long active fiber for signal generation and 20 m long

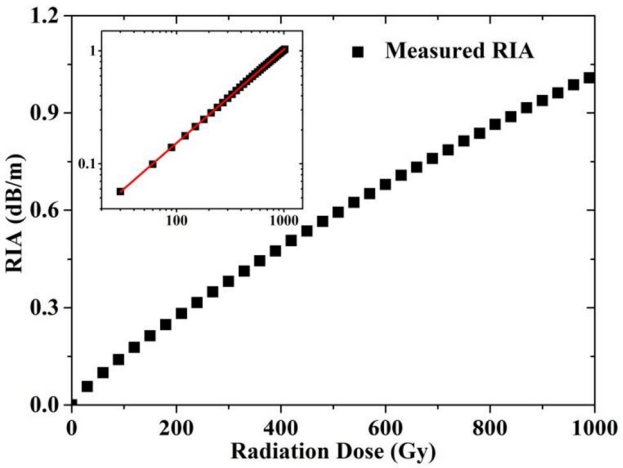


**Fig. 2** Measured RIA of the Yb-doped fiber at the laser wavelength. The inset shows the relationship between RIA and radiation dose in log–log scale

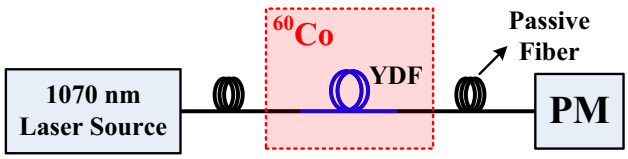


**Fig. 1** RIA measurement setup. *PM* power-meter

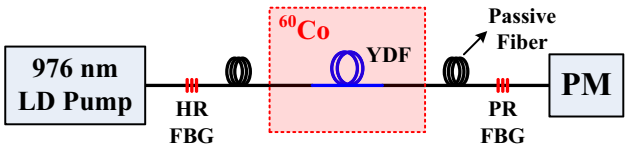


**Fig. 3** Schematic diagram of the radiation experiment. *HR* high reflectivity; *PR* partial reflectivity; *PM* power-meter

passive fiber for signal propagation. Exposed to a radiation dose rate of about 0.5 Gy/s, the Yb-doped fiber laser is examined every ~ 500 s during the radiation experiment to record the output power and efficiency.

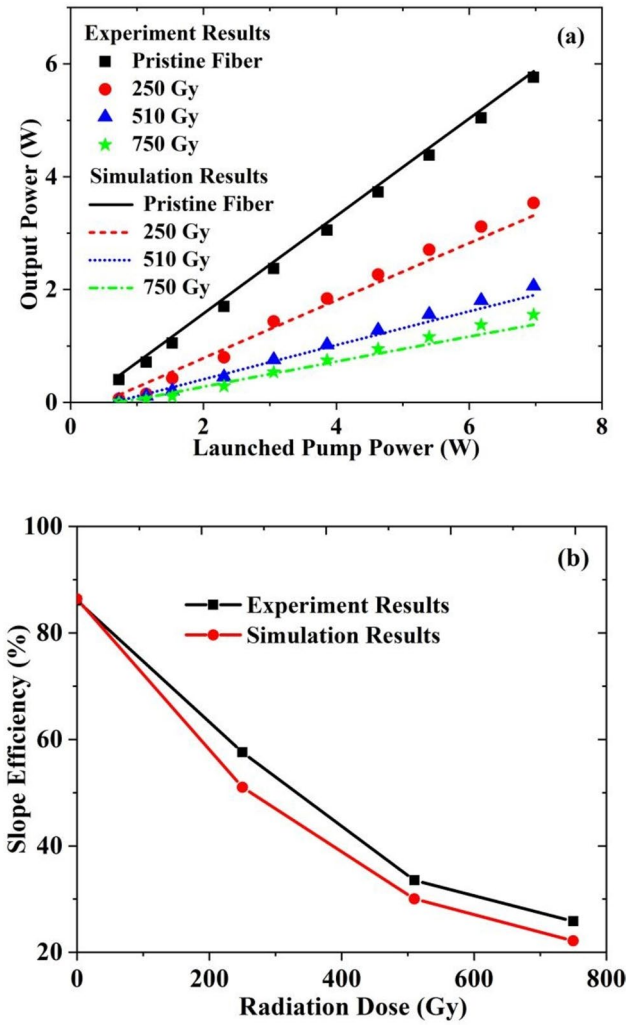


**Fig. 4** Output characteristics of the Yb-doped fiber laser in radiation: **a** output power; **b** slope efficiency

The output characteristics of the Yb-doped fiber laser at different radiation doses are given in Fig. 4. Figure 4a shows the output power of the laser as a function of the pump power. As can be seen, for a certain radiation level, the output still shows a linear relationship with the launched pump power. And this is consistent with the response of Yb-doped fiber amplifiers [12, 14, 28], Tm-doped fiber lasers [7–10] and Er-doped fiber amplifiers [5]. However, examined at a fixed pump, the output power drops dramatically with the accumulation of radiation dose, and, so does the operation efficiency of the laser system as shown in Fig. 4b, indicating that the intrinsic parameters of the active fiber vary with the radiation dose. For the investigated Yb-doped fiber laser, the slope efficiency experienced a remarkable decline from 86.1% at 0 Gy to 25.8% at 750 Gy. Besides, the threshold pump power witnessed a monotonous rise along with the radiation dose, demonstrating an increased loss inside of the cavity.

Corresponding simulation results are also depicted in Fig. 4 for comparison. In the simulation, the RIA at 1070 nm is taken from Eq. (5). Considering the close spectral location of the pump and the laser, RIA of the 976 nm pump is taken as the same. And, other parameters are listed in Table 1.

As can be found in Fig. 4, generally, the simulation results agree well with the experiments despite slight differences. For pristine fiber, the simulated output is very close to the experiments with a maximal power difference of about 0.15 W, while, for irradiated fiber, the simulated results are relatively smaller compared to the experiment results at high pump levels. This can be explained by the fact that, for every output power test with irradiated active fiber, the output is recorded with the pump power increasing step by step, introducing bleaching of the active fiber, and, consequently, leading to higher output powers at high pump levels. Even so, the maximal slope efficiency difference still keeps within 4%.

Above comparisons show that, the developed model is sufficient to correctly simulate the performance of the Yb-doped fiber laser in both pristine state and radiation state,

**Table 1** Physical parameters exploited in the simulation

| Parameter | Value | Parameter | Value |
|---|---|---|---|
| Doping concentration,$N$ | $6.36 \times 10^{25}$ m$^{-3}$ | Core radius,$r_1$ | 5 μm |
| RIC coefficient of the fiber core, $\kappa'_{co}$ | $3.23 \times 10^{-9}$ Gy$^{-1}$ [42] | Inner cladding radius,$r_2$ | 65 μm |
| RIC coefficient of the cladding,$\kappa'_{cl}$ | $0.62 \times 10^{-9}$ Gy$^{-1}$ [42] | Initial lifetime,$\tau_0$ | 900 μs |
| radiation-lifetime coefficient of Yb ions, $\gamma$ | − 0.102 [44] | Pump wavelength,$\lambda_p$ | 976 nm |
| absorption cross-section at the pump wavelength,$\sigma_{ap}$ | $2.47 \times 10^{-24}$ m$^{-3}$ | absorption cross-section at the laser wavelength,$\sigma_{as}$ | $3.93 \times 10^{-27}$ m$^{-3}$ |
| emission cross-section at the pump wavelength,$\sigma_{ep}$ | $2.44 \times 10^{-24}$ m$^{-3}$ | emission cross-section at the laser wavelength,$\sigma_{es}$ | $3.31 \times 10^{-25}$ m$^{-3}$ |

making it ready for optimization design of Yb-doped fiber laser systems in adverse environments.

## Optimization of Yb-doped fiber lasers with deposited radiation

In this part, the validated model is utilized to predict the system performance by varying the laser design, so as to optimize its configuration in radiation environments.

### Active fiber length and pump scheme

Firstly, impacts of active fiber length and pump scheme are investigated. And, Fig. 5 shows the output profiles of the laser system by varying the active fiber length and deposited radiation dose for three different pump schemes, namely forward pump scheme in Fig. 5a, bidirectional pump scheme in Fig. 5b and backward pump scheme in Fig. 5c, respectively. For the forward pump scheme, 10 W pump is injected from the opposite side to the laser output. And, most Yb-doped fiber lasers are built with this pump configuration. For the bidirectional pump scheme, 5 W pump is launched at each side of the active fiber, making a total pump power of 10 W. For the backward pump scheme, 10 W pump is injected from the laser output facet.

As can be seen in Fig. 5, the output power drops with the accumulation of radiation. And, faster decline is witnessed for longer active fiber which introduces higher extra propagation loss. For different pump schemes, generally, the backward pump scheme exhibits the highest lasing efficiency except for the high-radiation and long-active-fiber zone where the output power falls below 3 W, while the forward pump scheme shows the lowest output over the whole investigated area.

In the high-radiation and long-active-fiber zone, bidirectional pump scheme presents superior performance out of the three, thanks to a more even excited-state population distribution. However, in practices this would not be an option for radiation-resistant as the fiber length is way too long beyond the best choice, and, it has already been demonstrated that short active fibers with high doping concentrations are more favorable for adverse environment applications [30, 32, 34–36].

Besides, for different pump schemes and radiation dose, there always exists an optimal active fiber length which provides the highest output power. And, the optimal active fiber lengths and corresponding maximal output powers for different deposited radiation doses are plotted in Fig. 6. Here, the fiber length is varied with a step of 0.1 m which should be adequate for cavity optimization.

As shown in Fig. 6a, the optimal active fiber length shortens gradually with the accumulation of radiation. For all the three pump schemes, the optimal fiber length at 750 Gy is only about 50% of that at the pristine state. And, the backward pump scheme prefers a relatively longer active fiber compared with forward and bidirectional pump schemes. Variation of output powers at optimal active fiber lengths is depicted in Fig. 6b, which represents the slowest power decline curves in Fig. 5. For a deposited radiation of 750 Gy, the maximal outputs for the three different pump schemes all experience a shrink over 50%. For high power Yb-doped fiber laser systems, the output power deterioration would be even worse due to severe thermal effects induced by extra propagation loss [13, 14, 35, 36].

### Dynamic pump allocation

In practices, the active fiber length is set in the design phase, and, cannot be tuned during the laser operation process, limiting the overall optimization ability. In most cases, pump power can be easily manipulated through drive current control during operation, thus, for a given total pump power, varying the power allocation between the forward pump and the backward pump seems to be a more feasible way for radiation-resistance in practical applications.

Figure 7 presents the output profile of an Yb-doped fiber laser system with dynamic pump allocation. The 10 m active fiber is pumped from both sides with a total pump power of 10 W. As can be found, for a given radiation dose, especially at high radiation levels, with the increase of the forward pump power, the output power first rises and then decreases, demonstrating that there exists an optimal forward pump power which provides the highest operation efficiency. And, generally, a small forward pump power within 3 W is preferred.

The variation of the optimal forward pump power along with the radiation dose is given in Fig. 8. Here, the step size of the pump is set as 0.1 W, which is sufficient for power control in practice. As can be seen in Fig. 8, different from the optimal active fiber length in Fig. 6, which shortens monotonously with the accumulation of radiation, the optimal forward pump power takes a "V" shape. Within 100 Gy, the optimal forward pump decreases dramatically from 1.8 W to 0.8 W with the accumulation of radiation. And, beyond that, the optimal forward pump rises back gradually to about 2 W at 750 Gy.

Output powers at optimal forward pump are depicted in Fig. 9. And, comparison to systems with traditional pump schemes is also presented. Clearly, dynamic pump allocation provides the highest operation efficiency for different radiation levels. At low radiation doses within 200 Gy, backward pump scheme exhibits a comparable output. Over 200 Gy, with the increase of the radiation dose, the superiority of dynamic pump allocation becomes more and more evident. At 750 Gy, dynamic pump allocation witnesses a power

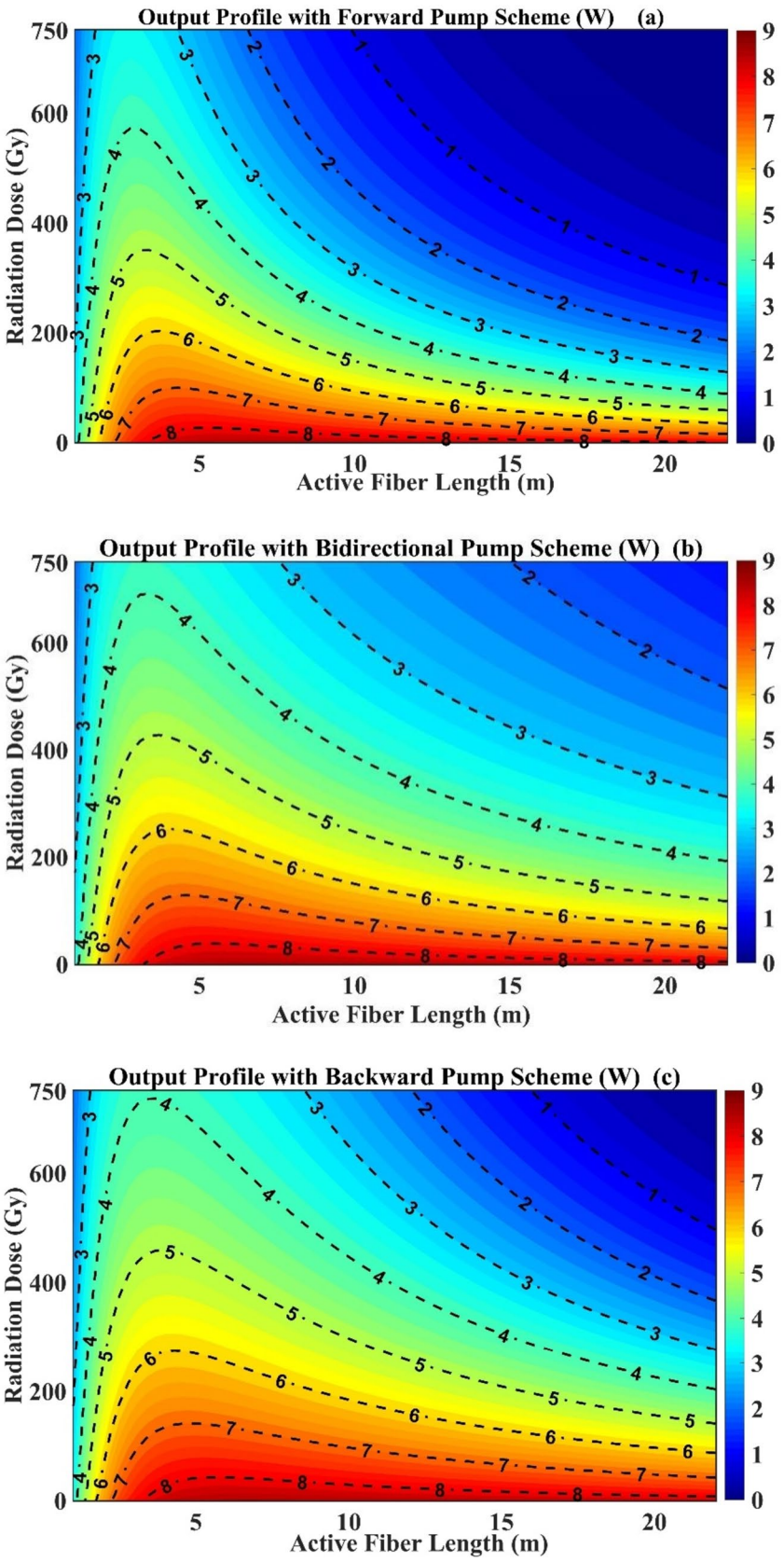


**Fig. 5** Output profiles at different active fiber lengths and radiation doses for three different pump schemes: **a** forward pump scheme; **b** bidirectional pump scheme; **c** backward pump scheme

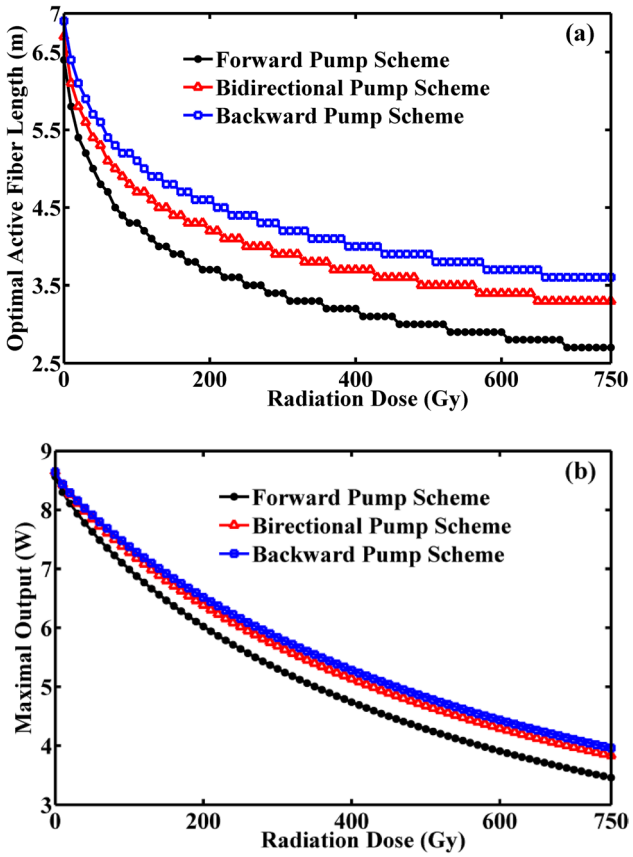


**Fig. 6** Optimal active fiber lengths and corresponding output powers for different pump schemes: **a** optimal active fiber lengths; **b** output powers at optimal active fiber lengths

decline of about 64.8% compared to 69.8% of the bidirectional pump and backward pump scheme. Even so, it still yields a tripled output power compared to that with forward pump scheme.

## Optimized design

The optimized design is achieved by combining the optimal active fiber length with dynamic pump allocation. Comparison between the optimized design and the traditional design is depicted in Fig. 10. Here, the total pump power is set at 10 W. For the traditional design, the most commonly used forward pump scheme is taken. And, the active fiber length is optimized at 6.4 m for the pristine state without radiation. For the optimized design, the active fiber length is optimized at 3.9 m for an expected total radiation dose of 500 Gy. And, the forward pump is varied along with the increase of the radiation dose.

As shown in Fig. 10, the laser output decays exponentially against the radiation dose. Below 20 Gy, the primary output of the traditional design is slightly larger than that of the optimized design. However, with a decay rate of $2.7\times10^{-3}$ Gy$^{-1}$, obtained through exponential decay fitting of the output curve, the output power of the traditional design presents a much faster decline. And, it falls quickly below the optimized design at around 20 Gy. Comparatively, the optimized design experiences a relatively slower output decline with a decay rate of $1.9\times10^{-3}$ Gy$^{-1}$, demonstrating improved radiation-resistance. At 750 Gy, the optimized design can alleviate the power degradation to about 3 dB instead of 6 dB for the traditional design by providing a doubled output power.

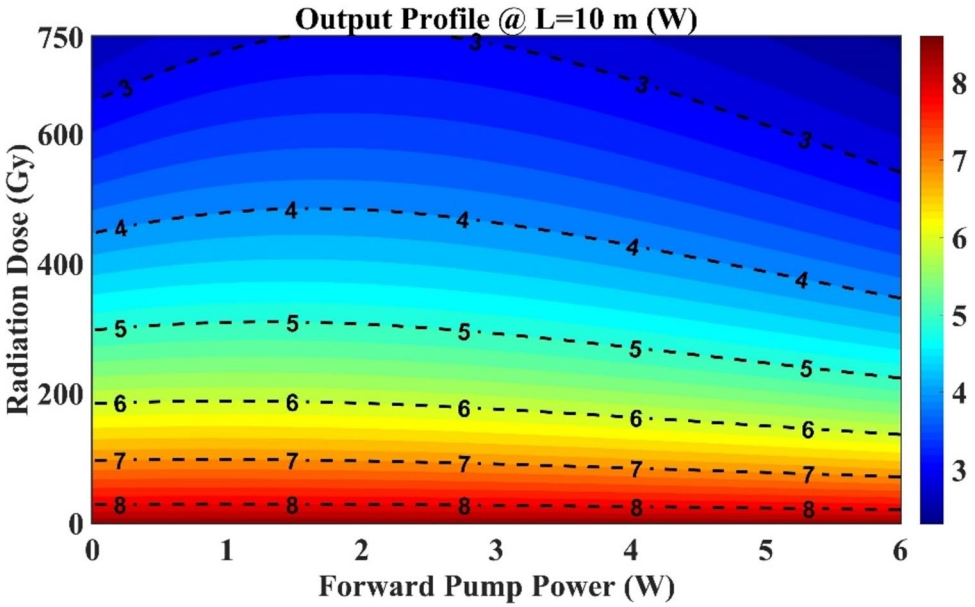


**Fig. 7** Output profile at different forward pump powers and radiation doses for a Yb-doped fiber laser system with 10 m active fiber

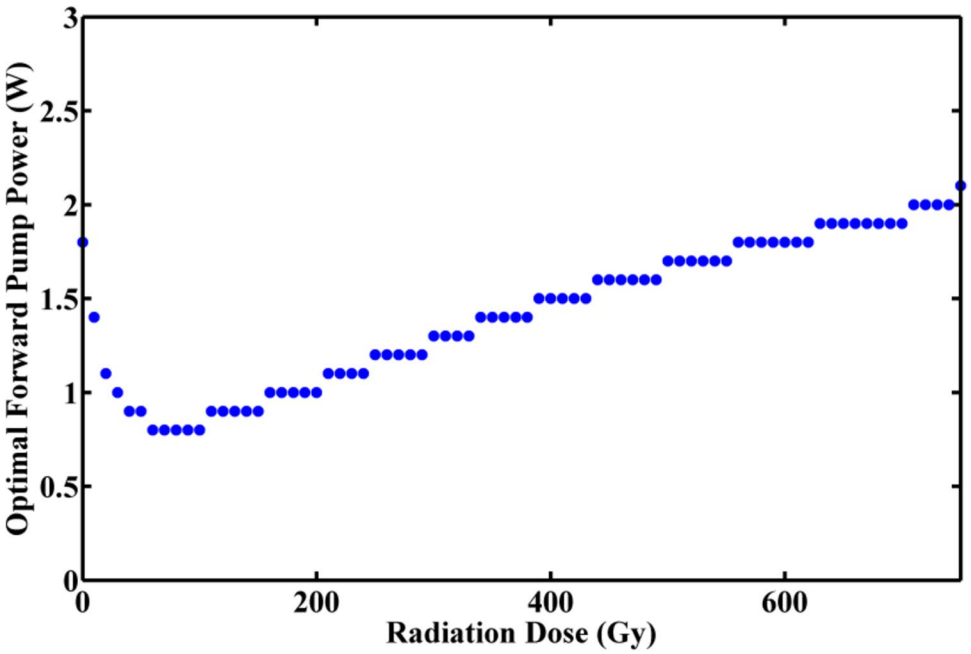


**Fig. 8** Variation of the optimal forward pump power against the radiation dose

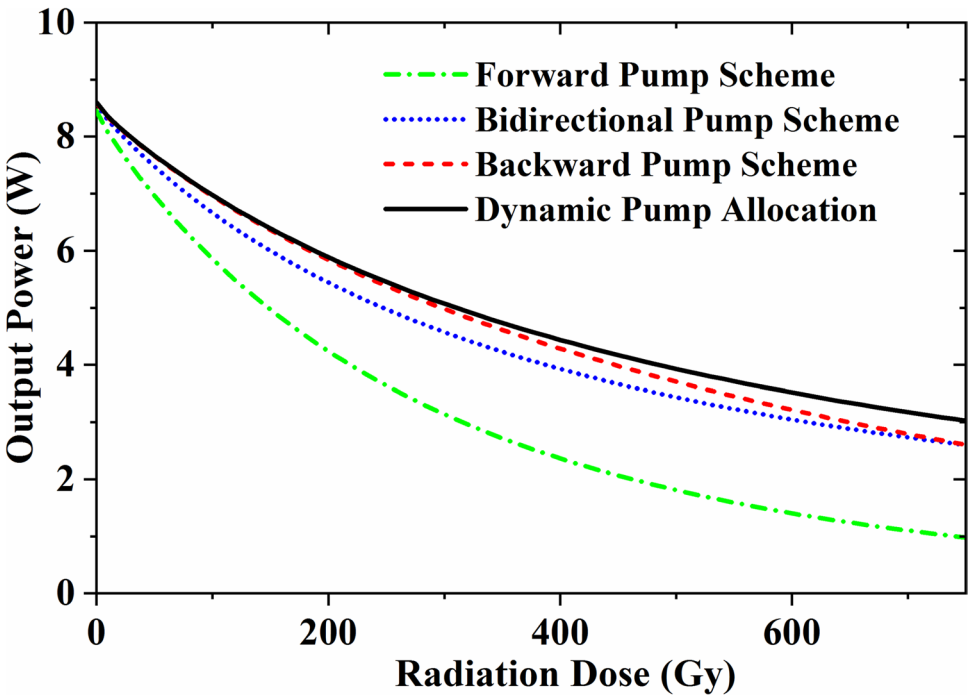


**Fig. 9** Comparison with traditional pump schemes

## Conclusions

To improve the radiation resistance of low- and moderate-power Yb-doped fiber lasers through architecture design, a simple radiation model is developed by introducing 3 primary radiation effects into the conventional fiber laser model. Comparisons with radiation experiments at different radiation levels up to 750 Gy show that this model is able to reproduce the laser behavior at both pristine state and radiation state, allowing it to predict the impacts of different design parameters on the radiation responses of the laser system. With this validated model, the influence of various design parameters on the laser performances is investigated. And, the optimized design for operation in radiation is attained, featuring short active fiber and dynamic pump allocation.

In practice, for any other Yb-doped laser systems, this radiation model could be ready for optimization application

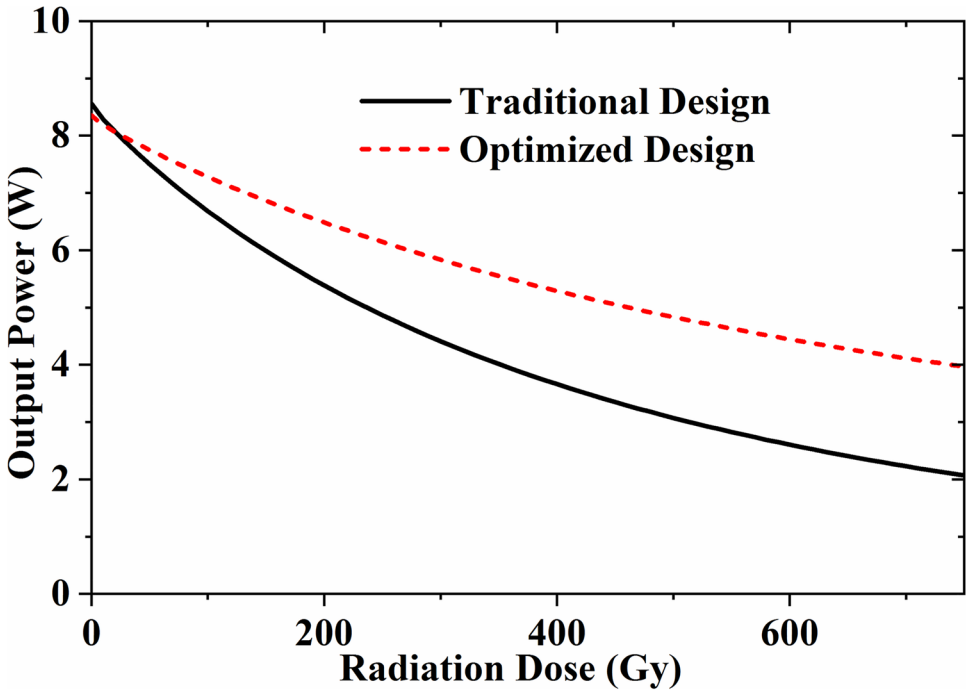


**Fig. 10** Comparisons between the radiation responses of optimized Yb-doped fiber lasers with and without consideration of radiation

with a very limited number of experimental tests, which provides the RIA data of the active fiber and basic validation. Besides, this paper fruther confirms that, aside from the traditional active hardening and bleaching methods, architecture optimization provides an efficient way for radiation tolerance alleviation of Yb-doped fiber lasers.

**Acknowledgements** This work is partially supported by the National Natural Science Foundation of China (Grant No. 62105268) and the State Key Laboratory of Laser Interaction with Matter (Grant No. SKLLIM2110). The authors would like to express their gratitude to Prof. Sheng Wang and Prof. Aiping Yi from the State Key Laboratory of Laser Interaction with Matter for their generous help during the manuscript preparation.



## References

1. Y. Cai, H. Liu, B. Liu, W. Lin, H. Zhang, Y. Qiao, Performance degradation and recovery of irradiated spaceborne fiber amplifier. Appl. Opt. **61**(4), 995–1000 (2022)
2. C. Shao, C. Yu, Y. Zhu, Q. Zhou, G. Boulon, M. Guzik, W. Chen, L. Hu, Radiation-induced color centers and their inhibition methods in Yb-doped silica fibers. J. Lumin. **248**, 118939 (2022)
3. S. Girard, A. Morana, A. Ladaci, T. Robin, L. Mescia, J. Bonnefois, M. Boutillier, J. Mekki, A. Paveau, B. Cadier, E. Marin, Y. Ouerdane, A. Boukenter, Recent advances in radiation-hardened fiber-based technologies for space applications. J. Opt. **20**, 093001 (2018)
4. J. Ma, M. Li, L. Tan, Y. Zhou, S. Yu, Q. Ran, Experimental investigation of radiation effect on erbium-ytterbium co-doped fiber amplifier for space optical communication in low-dose radiation environment. Opt. Express **17**(18), 15571–15577 (2009)
5. A. Ladaci, S. Girard, L. Mescia, A. Laurent, C. Ranger, D. Kermen, T. Robin, B. Cadier, M. Boutillier, B. Sane, E. Marin, A. Morana, Y. Ouerdane, A. Boukenter, Radiation hardened high-power $Er^{3+}/Yb^{3+}$-codoped fiber amplifiers for free-space optical communications. Opt. Lett. **43**(13), 3049–3052 (2018)
6. Y. Jiao, Q. Yang, Y. Zhu, F. Wang, L. Zhang, M. Wang, S. Wang, C. Shao, C. Yu, L. Hu, Improved radiation resistance of an Er-doped silica fiber by a preform pretreatment method. Opt. Express **30**(4), 6236–6247 (2022)
7. Y. Xing, H. Huang, N. Zhao, L. Liao, J. Li, N. Dai, Pump bleaching of Tm-dope d fiber with 793 nm pump source. Opt. Lett. **40**(5), 681–684 (2015)
8. Y. Xing, N. Zhao, L. Liao, Y. Wang, H. Li, J. Peng, L. Yang, N. Dai, J. Li, Active radiation hardening of Tm-doped silica fiber based on pump bleaching. Opt. Express **23**(19), 24236–24245 (2015)
9. Y. Xing, Y. Liu, N. Zhao, R. Cao, Y. Wang, Y. Yang, J. Peng, H. Li, L. Yang, N. Dai, J. Li, Radical passive bleaching of Tm-doped silica fiber with deuterium. Opt. Lett. **43**(5), 1075–1078 (2018)

10. Y. Xing, Y. Liu, R. Cao, L. Liao, Y. Chu, Y. Wang, J. Peng, H. Li, L. Yang, N. Dai, J. Li, Elimination of radiation damage in Tm-doped silica fibers based on the radical bleaching of deuterium loading. OSA Contin. **1**(3), 987–995 (2018)
11. B. Fox, K. Simmons-Potter, S. Moore, J. Fisher, D. Meister, Gamma-radiation-induced photodarkening in actively pumped Yb-doped optical fiber and investigation of post-irradiation transmittance recovery. Proc. SPIE **7434**, 74340C (2009)
12. S. Sun, L. Zhang, J. Dai, C. Gao, Y. Li, N. Liu, H. He, C. Shen, L. Jiang, F. Li, J. Lv, X. Zhou, W. Wu, Q. Zhang, B. Jia, P. Lu, J. Wang, Comparative study of γ-radiation resistance between Yb/Ce/F and Yb/P doped aluminosilicate fibers. Optik **250**, 168347 (2022)
13. Y. Wang, C. Gao, K. Peng, L. Ni, X. Wang, H. Zhan, Y. Li, L. Jiang, A. Lin, J. Wang, and F. Jing, "Laser performances of Yb-doped aluminophosphosilicate fiber under γ-radiation", Proc. 2018 Conference on Lasers and Electro-Optics Pacific Rim (CLEO-PR) p. F1B.2 (2018)
14. Y. Chen, H. Xu, Y. Xing, L. Liao, Y. Wang, F. Zhang, X. He, H. Li, J. Peng, L. Yang, N. Dai, J. Li, Impact of gamma-ray radiation-induced photodarkening on mode instability degradation of an ytterbium-doped fiber amplifier. Opt. Express **26**(16), 20430–20441 (2018)
15. C. Shao, C. Yu, Y. Jiao, G. Boulon, M. Guzik, L. Zhang, F. Lou, M. Wang, W. Chen, L. Hu, Radiation-induced darkening and its suppression methods in Yb-doped silica fiber core glasses. Int. J. Appl. Glass Sci. **13**, 457–475 (2022)
16. S. Girard, M. Vivona, A. Laurent, B. Cadier, C. Marcandella, T. Robin, E. Pinsard, A. Boukenter, Y. Ouerdane, Radiation hardening techniques for Er/Yb doped optical fibers and amplifiers for space application. Opt. Express **20**(8), 8457–8465 (2012)
17. C. Shao, W. Xu, N. Ollier, M. Guzik, G. Boulon, L. Yu, L. Zhang, C. Yu, S. Wang, L. Hu, Suppression mechanism of radiation-induced darkening by Ce doping in Al/Yb/Ce-doped silica glasses: evidence from optical spectroscopy, EPR and XPS analyses. J. Appl. Phys. **120**(15), 153101–153108 (2016)
18. C. Cao, Y. Xing, N. Dai, J. Li, Homemade radiation-resistant Er/Yb co-doped silica fiber for space applications in low and high-dose radiation environments. Proc. SPIE **12595**, 125951I (2023)
19. B. Wang, C. Cao, Z. Zhang, S. Liao, A. Zhang, X. Zhang, Y. Xing, G. Chen, J. Zhou, N. Dai, J. Peng, H. Li, J. Li, Investigation of radiation induced static mode degradation in Yb-Ce co-doped pulsed fiber amplifiers. Opt. Laser Technol. **154**, 108345 (2022)
20. C. Shao, F. Wang, M. Guo, J. Yang, H. Zhang, J. Li, S. Wang, C. Yu, J. Ren, L. Hu, Structure and property of $Yb^{3+}$/$Al^{3+}$/$Ce^{3+}$/F–doped silica glasses. J. Chin. Ceram. Soc. **47**(1), 120–131 (2019)
21. K. Zotov, M. Likhachev, A. Tomashuk, M. Bubnov, M. Yashkov, A. Guryanov, Radiation-resistant erbium-doped silica fibre. Quantum Electron **37**(10), 946–949 (2007)
22. S. Girard, A. Laurent, E. Pinsard, T. Robin, B. Cadier, M. Boutillier, C. Marcandella, A. Boukenter, Y. Ouerdane, Radiation-hard erbium optical fiber and fiber amplifier for both low- and high-dose space missions. Opt. Lett. **39**(9), 2541–2544 (2014)
23. M. Vivona, S. Girard, C. Marcandella, T. Robin, B. Cadier, M. Cannas, A. Boukenter, Y. Ouerdane, Influence of Ce codoping and $H_2$ pre-loading on Er/Yb-doped fiber: radiation response characterized by confocal micro-luminescence. J. Non-Cryst. Solids **357**, 1963–1965 (2011)
24. M. Likhachev, M. Bubnov, K. Zotov, A. Tomashuk, D. Lipatov, M. Yashkov, Radiation resistance of Er-doped silica fibers: effect of host glass composition. J. Lightwave Technol. **31**(5), 749–755 (2013)
25. C. Shao, J. Ren, F. Wang, N. Ollier, F. Xie, X. Zhang, L. Zhang, C. Yu, L. Hu, Origin of radiation-induced darkening in $Yb^{3+}$/$Al^{3+}$/$P^{5+}$-doped silica glasses: effect of the P/Al ratio. J. Phys. Chem. B **122**(10), 2809–2820 (2018)
26. B. Babu, N. Ollier, I. Savelli, H. Hamzaoui, A. Pastouret, B. Poumellec, M. Bouazaoui, L. Bigot, M. Lancry, Study of radiation effects on $Er^{3+}$-doped nanoparticles germano-silica fibers. J. Lightwave Technol. **34**(21), 4981–4987 (2016)
27. A. Yeniay, R. Gao, Radiation induced loss properties and hardness enhancement technique for Er/Yb doped fibers for avionic applications. Opt. Fiber Technol. **19**(2), 88–92 (2013)
28. X. Wang, S. Sun, Y. Zheng, M. Yu, S. Li, Y. Cao, J. Wang, Influence of pre-radiation and photo-bleaching on the Yb-doped fiber laser radiated with gamma-ray. Appl. Sci. **13**, 6146 (2023)
29. O. Berne, M. Caussanel, O. Gilard, A model for the prediction of EDFA gain in a space radiation environment. IEEE Photonics Technol. Lett. **16**(10), 2227–2229 (2004)
30. S. Girard, L. Mescia, M. Vivona, A. Laurent, Y. Ouerdane, C. Marcandella, F. Prudenzano, A. Boukenter, T. Robin, P. Paillet, V. Goiffon, M. Gaillardin, B. Cadier, E. Pinsard, M. Cannas, R. Boscaino, Design of radiation-hardened rare-earth doped amplifiers through a coupled experiment/simulation approach. J. Lightwave Technol. **31**(8), 1247–1254 (2013)
31. L. Mescia, S. Girard, P. Bia, T. Robin, A. Laurent, F. Prudenzano, A. Boukenter, Y. Ouerdane, Optimization of the design of high power Er/Yb-codoped fiber amplifiers for space missions by means of particle swarm approach. IEEE J. Sel. Topics Quantum Electron. **20**(5), 3100108 (2014)
32. A. Ladaci, S. Girard, L. Mescia, T. Robin, A. Laurent, B. Cadier, M. Boutillier, Y. Ouerdane, A. Boukenter, Optimized radiation-hardened erbium doped fiber amplifiers for long space missions. J. Appl. Phys. **121**, 163104 (2017)
33. L. Mescia, P. Bia, S. Girard, A. Ladaci, M.A. Chiapperino, T. Robin, A. Laurent, B. Cadier, M. Boutillier, Y. Ouerdane, A. Boukenter, Temperature-dependent modeling of cladding-pumped Er/Yb codoped fiber amplifiers for space applications. J. Lightwave Technol. **36**(17), 3594–3602 (2018)
34. C. Campanella, L. Mescia, P. Bia, M.A. Chiapperino, S. Girard, T. Robin, J. Mekki, E. Marin, A. Boukenter, Y. Ouerdane, Theoretical investigation of thermal effects in high power Er/Yb codoped double-clad fiber amplifiers for space applications. Phys. Status Solidi A **216**, 1800582 (2018)
35. M. Tao, H. Chen, G. Feng, K. Luan, F. Wang, K. Wang, X. Ye, Thermal modeling of high-power Yb-doped fiber lasers with irradiated active fibers. Opt. Express **28**(7), 10104–10123 (2020)
36. M. Tao, H. Chen, G. Feng, L. Wang, J. Ye, Y. Wang, X. Ye, W. Chen, Comparisons of high power fiber systems in the presence of radiation induced photodarkening. Laser Phys. **32**, 055101 (2022)
37. I. Kelson, A. Hardy, Strongly pump fiber lasers. IEEE J. Quantum Electron. **34**(9), 1570–1577 (1998)
38. I. Kelson, A. Hardy, Optimization of strongly pumped fiber lasers. J. Lightwave Technol. **17**(5), 891–897 (1999)
39. S. Girard, J. Kuhnhenn, A. Gusarov, B. Brichard, M. Van Uffelen, Y. Ouerdane, A. Boukenter, C. Marcandella, Radiation effects on silica-based optical fibers: recent advances and future challenges. IEEE T. Nucl. Sci. **60**(3), 2015–2036 (2003)
40. A.F. Fernandez, B. Brichard, F. Berghmans, In situ measurement of refractive index changes induced by gamma radiation in germanosilicate fibers. IEEE Photo. Technol. Lett. **15**(10), 1428–1430 (2003)
41. D. Hand, P. Russell, Photoinduced refractive-index changes in germanosilicate fibers. Opt. Lett. **15**(2), 102–104 (1990)
42. S. Kher, S. Chaubey, S.M. Oak, A. Gusarov, Measurement of γ-radiation induced refractive index changes in B/Ge doped fiber using LPGs. IEEE Photon. Technol. Lett. **25**(21), 2070–2073 (2013)
43. D. Marcuse, Gaussian approximation of the fundamental modes of garded-index fibers. J. Opt. Soc. Am. **68**(1), 103–109 (1978)
44. A. Ladaci, S. Girard, L. Mescia, T. Robin, A. Laurent, B. Cadier, M. Boutillier, A. Morana, D.D. Francesca, Y. Ouerdane, A.

Boukenter, X-rays, γ -rays, electrons and protons radiation-induced changes on the lifetimes of Er and Yb ions in silica-based optical fibers. J. Lumin. **195**, 402–407 (2018)
45. V. Pukhkaya, P. Goldner, A. Ferrier, N. Ollier, Impact of rare earth element clusters on the excited state lifetime evolution under irradiation in oxide glasses. Opt. Express **23**(3), 3270–3281 (2015)